Wavelength-Multiplexed Beam Steering in Fiber and Visible Light Communication Integrated Indoor Access Network

Wenqing Niu, Fujie Li, Zengyi Xu, Chao Shen, Ziwei Li, Jianyang Shi, Junwen Zhang, and Nan Chi*
Key Laboratory for Information Science of Electromagnetic Waves (MoE), Fudan University, Shanghai 200433, China.
*nanchi@fudan.edu.cn

Abstract: We propose a wavelength-multiplexed fiber and VLC integrated access network. Neural networks with a generator-model structure are employed for single-hologram-based wavelength-multiplexed beam steering. A 2λ transmission with overall data rate of 4.02 Gbps is demonstrated.

1. Introduction

With the development of mobile communication and internet of things (IoT), the demand for high-speed indoor wireless access networks is increasing rapidly. Visible light communication (VLC) has become a promising candidate owing to its broad unlicensed spectrum resources [1]. The use of spatial light modulator (SLM) or optical phase arrays with multimode fibers (MMF) or plastic optical fibers (POF) for beam steering becomes popular [2]–[4] as it's compatible to the optical distribution networks. Wavelength-division-multiplexed (WDM) fiber and VLC integrated access networks are expected to provide multiuser access. However, the output of MMF displays a mixture of speckles due to mode coupling and scattering [5]. To tackle with the interchannel crosstalk, wavefront manipulation techniques have been developed to achieve confined illumination towards the user. However, for multiuser access, previous researches require precise alignment to the divided regions of SLM [6] or switching the holograms to steer beams of different wavelengths [7]. Simultaneous transmission for multiuser remains a challenging task.

In this work, we propose a wavelength-multiplexed fiber and VLC integrated access network. The concept diagram is shown in Fig.1 (a). Neural networks with a generator-model structure are proposed for single-hologram-based wavelength-multiplexed beam steering for the first time. The model networks (MNets) learn the forward propagation process of the system, while the wavelength-multiplexed generator network (WM-GNet) learns the inverse process and generates the hologram for beam steering. Experimental results indicate that the proposed method can manipulate the beam of two wavelengths simultaneously and significantly suppress interchannel crosstalk. A 2-λ transmission with the overall data rate of 4.02 Gbps is achieved without extra spectral splitting or spatial focusing at the receiver.

2. Methods and Experimental setup

The principle of the proposed algorithm is shown in Fig. 1 (b). Two wavelengths (λ_1 is red and λ_2 is green) are taken for example. Two MNets and a WM-GNet are employed for the wavelength-multiplexed beam steering task. There are four main steps. First, random SLM holograms and the corresponding speckle patterns of the two wavelengths after MMF transmission are zipped as training data. Second, the $\lambda_1$and λ_2 MNets are trained independently using the training data set. The third step is WM-GNet training. The parameters of the two MNets are fixed. The input of WM-GNet is the target intensity diagrams after beam steering, and the output of GNet is predicted single hologram, which is used as input of the λ_1 and λ_2 MNets. Finally, the predicted SLM hologram is sent through the system to acquire the desired beam steering.

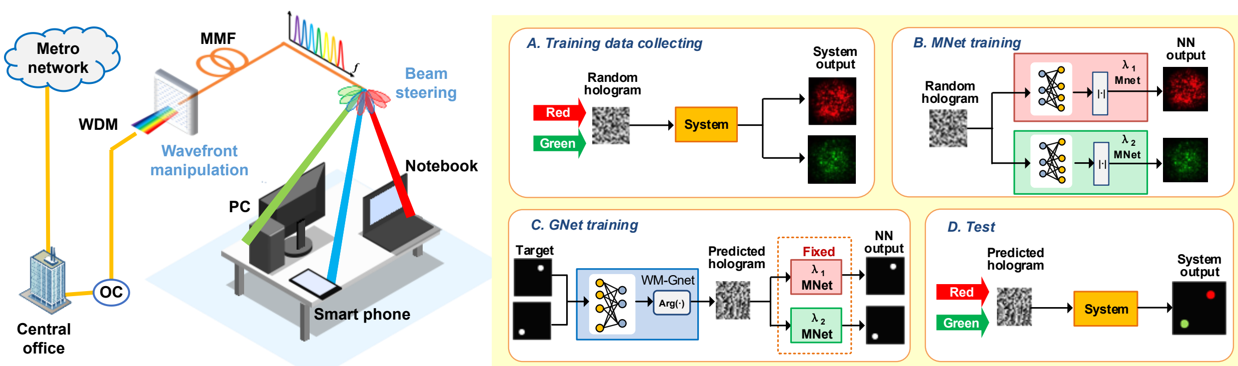

(a) (b)

Fig. 1. (a) Concept of the wavelength-multiplexed fiber and VLC integrated indoor access network. (b) Principle of proposed model-generator neural networks for wavelength-multiplexed single hologram beam steering.

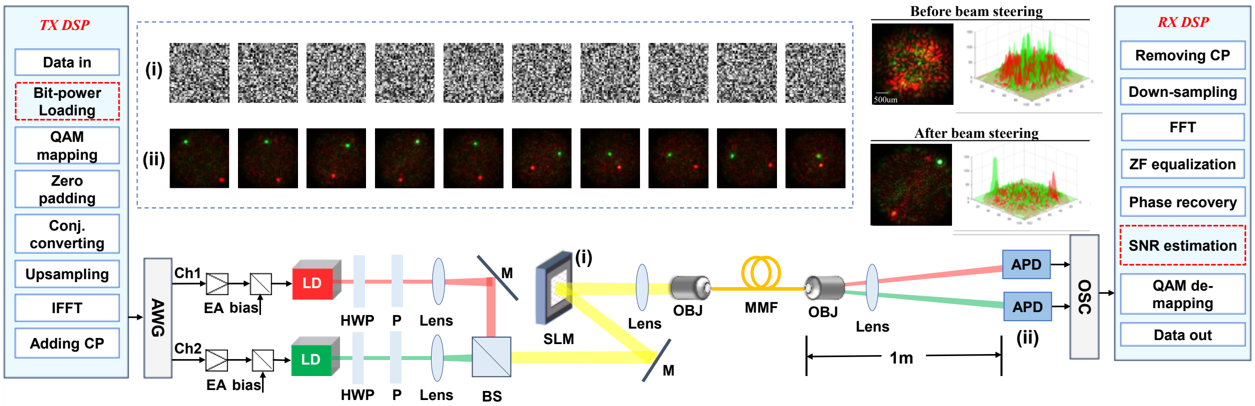

Fig. 2. Experimental setup of the wavelength multiplexed fiber and VLC integrated system. insets (i) and (ii) are phase patterns on the SLM and the corresponding wavelength multiplexed beam forming results respectively.

The design of MNets follows the physical propagation in MMF, the diffraction in free space, and intensity detection of the receiver, which includes the phase-to-complex-value conversion, a simple complex-valued fully-connected layer without bias terms [8], and the norm operation. Hence, the MNets are scalable and have misalignment tolerance. WM-GNet includes a simple complex-valued fully-connected layer and argument function. The input of the networks is flattened to 1-dimensional tensor and the output is reshaped into 2-dimensional tensor. The loss functions for MNets and GNet are mean square error (MSE) and the logarithm of the Pearson's coefficient [9], respectively.

The experimental setup is illustrated in Fig.2. Bit and power loading (BPL) discrete multitone (DMT) modulation algorithm is employed, including two steps: signal-to-noise ratio (SNR) estimation and BPL [10]. The subblock with solid lines are common in the two steps, while the dash lines denote the unique operations. First, the SNR of each subcarrier is estimated by transmitting QPSK signals. Then bit and power ratio are allocated according to the SNR and bit error rate (BER) threshold. Next, the bit sequences are mapped to QAM sequences. After DMT modulation, the digital signals are converted to analog signals by an arbitrary waveform generator (AWG, Agilent 8190A). The data for channel 1 and channel 2 are independent and transmitted simultaneously. After amplified by the electrical amplifiers (EAs), the signals are coupled with the direct current by the bias-Tees to drive the laser diodes (LDs). A red LD (OSRAM, 638nm) and a green LD (OSRAM, 520nm) are used as transmitters. Halfwave plates and polarizers are used to adjust the polarization states and optical power. Lenses are employed for collimation. Then, a beam splitter is employed to combine the two beams. Insets (i) in Fig. 2 are the generated holograms on SLM (PLUTO-2.1-VIS-014). Then the modulated beams are coupled into the MMF (SI-50um-0.22NA) by the objective lens and tube lens. Another objective lens and tube lens are employed at the distal end of the MMF.

After 1-m free space transmission, the APD (Menlo systems, APD210) is used to convert the optical signal to electrical signal. The wavelength multiplexed beam steering results are displayed in insets (ii). It's observed that the beam can be steered to arbitrary positions precisely by generating the corresponding phase patterns using the WM-GNet. The intensity of the MMF output before and after beam steering are also displayed in Fig. 2. It's clear that before beam steering, the intensity maps of the two wavelengths are mixed. Thus, there are strong inter-channel interference for the two channels. In contrast, the intensity maps after beam steering indicate that there are distinct peaks at the desired positions. Notably, the steerable angle range is limited by the field of view of camera in this experiment. The oscilloscope (OSC, MSO9254A) is used for analog-to-digital conversion. Then DMT demodulation and ZF equalization is employed to recover the signals. The two channels are de-modulated and decoded independently.

3. Results and Discussion

The achievable information rate (AIR) of channel 1 (λ_1 =638 nm) versus V_{pp} of the two channels before and after beam steering are shown in Fig. 3 (a) and (c), while the AIR of channel 2 (λ_2 =520 nm) versus V_{pp} of the two channels before and after beam steering are shown in Fig. 3 (b) and (d). For cases before beam steering, the AIR of one channel is severely influenced by the V_{pp} of another channel because of the severe interchannel crosstalk. Additionally, although we ensure that the output optical powers of the two channels are identical, the performance of the two channels are different because the responsivity at the two wavelengths. As a result, simultaneous high-speed transmission for the two channels is impossible if there is no filter at the receiver, especially for channel 2 (λ_2 =520 nm). In contrast, the single-hologram-based wavelength-multiplexed beam steering works well. For each channel,

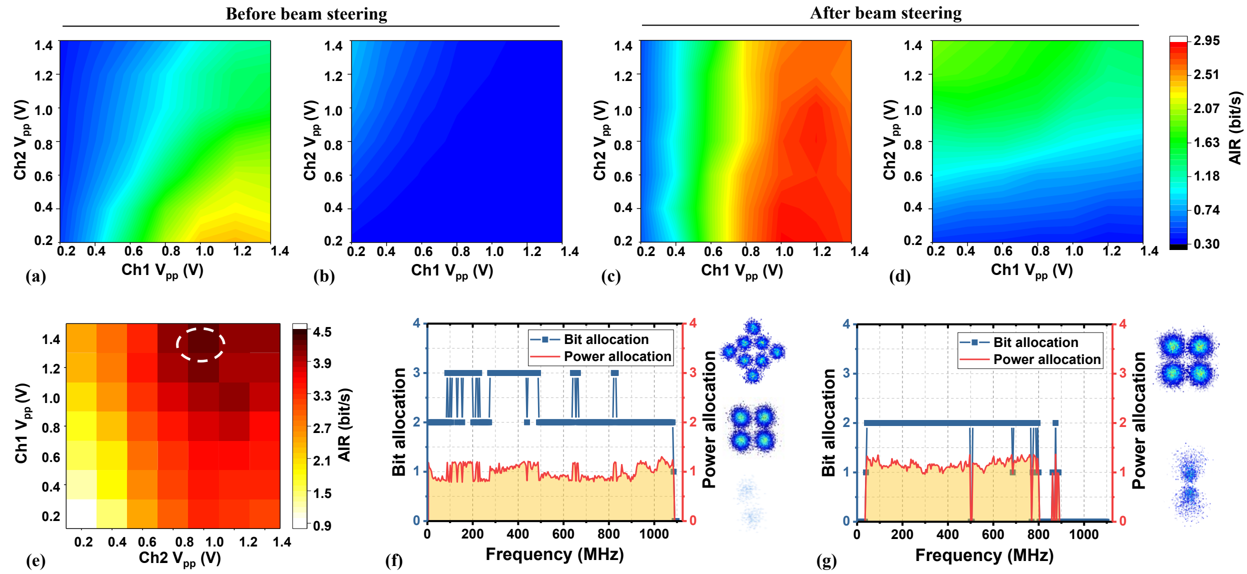

Fig. 3. (a) and (b) are the AIR results versus Vpp of λ_1 and λ_2 before beam steering. (c) and (d) are the AIR results versus Vpp of λ_1 and λ_2 after beam steering. (e) The total AIR versus the Vpp of the two channels. (f) and (g) are BPL results of λ_1 and λ_1 at the operating Vpp points (1V, 1.4V).

most of the optical power is directed to the desired position. Thus, the crosstalk from another channel can be suppressed. As a result, it's possible for the two channels to transmit high-speed data simultaneously.

The total AIR versus the V_{pp} of the two channels with single-hologram-based wavelength-multiplexed beam steering is shown in Fig. 3 (e). We find the highest AIR is achieved at the operating point (1V, 1.4V). It should be noted that higher V_{pp} not corresponds to better performance because nonlinear effect also becomes stronger. Fig. 3 (f) and (g) are the bit and power allocation results of channel 1 (λ_1 =638 nm) and channel 2 (λ_2 =520 nm) respectively. The constellation diagrams of the received signals are also inserted in Fig. 3. It's observed that channel 1 (λ_1 =638 nm) has higher SNR and modulation bandwidth than channel 2 (λ_2 =520 nm). Under the HD-FEC threshold of 3.8×10^{-3}, the data rates of channel 1 and channel 2 are 2.52 Gbps and 1.50 Gbps, respectively. In summary, the overall data rate exceeds 4.02 Gbps.

4. Conclusion

In this paper, we propose a wavelength-multiplexed fiber and VLC integrated access network, and experimentally demonstrate a 2-λ multiplexed system using red (λ_1 =638 nm) and green (λ_2 =520 nm) lasers for example. Neural networks with a generator-model structure are employed for single-hologram-based wavelength-multiplexed beam steering. The single hologram can steer the beam of two wavelengths simultaneously. Thus, the interchannel interference can be suppressed significantly. After 1-m free space VLC transmission, the overall data rate exceeds 4.02 Gbps.

Acknowledgements

This research is funded by the National Key Research and Development Program of China (2022YFB2802803), and the Natural Science Foundation of China Project (No. 61925104, No. 62031011, No. 62201157).

5. Reference

[1] N. Chi, H. Haas, M. Kavehrad, T. D. C. Little, and X. L. Huang, *IEEE Wirel. Commun.*, vol. 22, no. 2, pp. 5–7, 2015.
[2] C. R. B. Corrêa, A. M. J. Koonen, and E. Tangdiongga, *OFC 2023.*, pp. 4–6, 2023.
[3] D. C. O'Brien, in *Broadband Access Communication Technologies XIII*, Feb. 2019, no. February 2019, p. 19.
[4] Z. Cao *et al.*, *Opt. InfoBase Conf. Pap.*, pp. 1–3, 2022.
[5] N. Borhani, E. Kakkava, C. Moser, and D. Psaltis, *Optica*, vol. 5, no. 8, p. 960, 2018.
[6] X. Zhou, J. Shi, N. Chi, C. Shen, and Z. Li, *Opt. Express*, vol. 31, no. 16, p. 25359, 2023.
[7] Y. Wu and Z. Zhang, *Int. Conf. Commun. Technol. Proceedings, ICCT*, vol. 2022-Novem, pp. 322–326, 2022,.
[8] J. Wang, G. Zhong, D. Wu, S. Huang, Z.-C. Luo, and Y. Shen, *Opt. Express*, vol. 31, no. 3, p. 4839, Jan. 2023.
[9] B. Rahmani *et al.*, *Nat. Mach. Intell.*, vol. 2, no. 7, pp. 403–410, 2020.
[10] F. Hu *et al.*, *PhotoniX*, vol. 2, no. 16, p. 1581, 2021.